

Observation of Cabibbo Suppressed $B \rightarrow D^{(*)}K^-$ Decays at Belle

K. Abe,¹⁰ K. Abe,³⁷ I. Adachi,¹⁰ Byoung Sup Ahn,¹⁵ H. Aihara,³⁸ M. Akatsu,²⁰ G. Alimonti,⁹ Y. Asano,⁴³ T. Aso,⁴² V. Aulchenko,² T. Aushev,¹³ A. M. Bakich,³⁴ W. Bartel,^{6,10} S. Behari,¹⁰ P. K. Behera,⁴⁴ D. Beilene,² A. Bondar,² A. Bozek,¹⁶ T. E. Browder,⁹ B. C. K. Casey,⁹ P. Chang,²⁴ Y. Chao,²⁴ B. G. Cheon,³³ S.-K. Choi,⁸ Y. Choi,³³ S. Eidelman,² Y. Enari,²⁰ R. Enomoto,^{10,11} F. Fang,⁹ H. Fujii,¹⁰ C. Fukunaga,⁴⁰ M. Fukushima,¹¹ A. Garmash,^{2,10} A. Gordon,¹⁸ K. Gotow,⁴⁵ R. Guo,²² J. Haba,¹⁰ H. Hamasaki,¹⁰ K. Hanagaki,³⁰ F. Handa,³⁷ K. Hara,²⁸ T. Hara,²⁸ N. C. Hastings,¹⁸ H. Hayashii,²¹ M. Hazumi,²⁸ E. M. Heenan,¹⁸ I. Higuchi,³⁷ T. Higuchi,³⁸ H. Hirano,⁴¹ T. Hojo,²⁸ Y. Hoshi,³⁶ W.-S. Hou,²⁴ S.-C. Hsu,²⁴ H.-C. Huang,²⁴ Y. Igarashi,¹⁰ T. Iijima,¹⁰ H. Ikeda,¹⁰ K. Inami,²⁰ A. Ishikawa,²⁰ H. Ishino,³⁹ R. Itoh,¹⁰ G. Iwai,²⁶ H. Iwasaki,¹⁰ Y. Iwasaki,¹⁰ D. J. Jackson,²⁸ P. Jalocho,¹⁶ H. K. Jang,³² M. Jones,⁹ R. Kagan,¹³ H. Kakuno,³⁹ J. Kaneko,³⁹ J. H. Kang,⁴⁶ J. S. Kang,¹⁵ N. Katayama,¹⁰ H. Kawai,³ H. Kawai,³⁸ T. Kawasaki,²⁶ H. Kichimi,¹⁰ D. W. Kim,³³ Heejong Kim,⁴⁶ H. J. Kim,⁴⁶ Hyunwoo Kim,¹⁵ S. K. Kim,³² K. Kinoshita,⁵ S. Kobayashi,³¹ P. Krokovny,² R. Kulasiri,⁵ S. Kumar,²⁹ A. Kuzmin,² Y.-J. Kwon,⁴⁶ J. S. Lange,⁷ M. H. Lee,¹⁰ S. H. Lee,³² D. Liventsev,¹³ R.-S. Lu,²⁴ D. Marlow,³⁰ T. Matsubara,³⁸ S. Matsumoto,⁴ T. Matsumoto,²⁰ K. Miyabayashi,²¹ H. Miyake,²⁸ H. Miyata,²⁶ G. R. Moloney,¹⁸ S. Mori,⁴³ T. Mori,⁴ A. Murakami,³¹ T. Nagamine,³⁷ Y. Nagasaka,¹⁹ T. Nakadaira,³⁸ E. Nakano,²⁷ M. Nakao,¹⁰ J. W. Nam,³³ S. Narita,³⁷ K. Neichi,³⁶ S. Nishida,¹⁷ O. Nitoh,⁴¹ S. Noguchi,²¹ T. Nozaki,¹⁰ S. Ogawa,³⁵ T. Ohshima,²⁰ T. Okabe,²⁰ S. Okuno,¹⁴ S. L. Olsen,⁹ H. Ozaki,¹⁰ P. Pakhlov,¹³ H. Palka,¹⁶ C. S. Park,³² C. W. Park,¹⁵ H. Park,¹⁵ L. S. Peak,³⁴ M. Peters,⁹ L. E. Piilonen,⁴⁵ J. L. Rodriguez,⁹ N. Root,² M. Rozanska,¹⁶ K. Rybicki,¹⁶ J. Ryuko,²⁸ H. Sagawa,¹⁰ Y. Sakai,¹⁰ H. Sakamoto,¹⁷ M. Satapathy,⁴⁴ A. Satpathy,^{10,5} S. Schrenk,⁵ S. Semenov,¹³ K. Senyo,²⁰ M. E. Sevier,¹⁸ H. Shibuya,³⁵ B. Shwartz,² V. Sidorov,² J. B. Singh,²⁹ S. Stanič,⁴³ A. Sugi,²⁰ A. Sugiyama,²⁰ K. Sumisawa,²⁸ T. Sumiyoshi,¹⁰ J.-I. Suzuki,¹⁰ K. Suzuki,³ S. Suzuki,²⁰ S. Y. Suzuki,¹⁰ S. K. Swain,⁹ T. Takahashi,²⁷ F. Takasaki,¹⁰ M. Takita,²⁸ K. Tamai,¹⁰ N. Tamura,²⁶ J. Tanaka,³⁸ M. Tanaka,¹⁰ G. N. Taylor,¹⁸ Y. Teramoto,²⁷ M. Tomoto,²⁰ T. Tomura,³⁸ S. N. Tovey,¹⁸ K. Trabelsi,⁹ T. Tsuboyama,¹⁰ T. Tsukamoto,¹⁰ S. Uehara,¹⁰ K. Ueno,²⁴ Y. Unno,³ S. Uno,¹⁰ Y. Ushiroda,^{17,10} Y. Usov,² S. E. Vahsen,³⁰ G. Varner,⁹ K. E. Varvell,³⁴ C. C. Wang,²⁴ C. H. Wang,²³ J. G. Wang,⁴⁵ M.-Z. Wang,²⁴ Y. Watanabe,³⁹ E. Won,³² B. D. Yabsley,¹⁰ Y. Yamada,¹⁰ M. Yamaga,³⁷ A. Yamaguchi,³⁷ H. Yamamoto,⁹ Y. Yamashita,²⁵ M. Yamauchi,¹⁰ S. Yanaka,³⁹ M. Yokoyama,³⁸ K. Yoshida,²⁰ Y. Yusa,³⁷ H. Yuta,¹ C. C. Zhang,¹² J. Zhang,⁴³ H. W. Zhao,¹⁰ Y. Zheng,⁹ V. Zhilich,² and D. Žontar⁴³

(Belle Collaboration)

¹Aomori University, Aomori

²Budker Institute of Nuclear Physics, Novosibirsk

³Chiba University, Chiba

⁴Chuo University, Tokyo

⁵University of Cincinnati, Cincinnati, Ohio

⁶Deutsches Elektronen-Synchrotron, Hamburg

⁷University of Frankfurt, Frankfurt

⁸Gyeongsang National University, Chinju

⁹University of Hawaii, Honolulu, Hawaii

¹⁰High Energy Accelerator Research Organization (KEK), Tsukuba

¹¹Institute for Cosmic Ray Research, University of Tokyo, Tokyo

¹²Institute of High Energy Physics, Chinese Academy of Sciences, Beijing

¹³Institute for Theoretical and Experimental Physics, Moscow

¹⁴Kanagawa University, Yokohama

¹⁵Korea University, Seoul

¹⁶H. Niewodniczanski Institute of Nuclear Physics, Krakow

¹⁷Kyoto University, Kyoto

¹⁸University of Melbourne, Victoria

¹⁹Nagasaki Institute of Applied Science, Nagasaki

²⁰Nagoya University, Nagoya

²¹Nara Women's University, Nara

²²National Kaohsiung Normal University, Kaohsiung

²³National Lien-Ho Institute of Technology, Miao Li

²⁴National Taiwan University, Taipei

²⁵Nihon Dental College, Niigata

²⁶Niigata University, Niigata

²⁷Osaka City University, Osaka²⁸Osaka University, Osaka²⁹Panjab University, Chandigarh³⁰Princeton University, Princeton, New Jersey³¹Saga University, Saga³²Seoul National University, Seoul³³Sungkyunkwan University, Suwon³⁴University of Sydney, Sydney NSW³⁵Toho University, Funabashi³⁶Tohoku Gakuin University, Tagajo³⁷Tohoku University, Sendai³⁸University of Tokyo, Tokyo³⁹Tokyo Institute of Technology, Tokyo⁴⁰Tokyo Metropolitan University, Tokyo⁴¹Tokyo University of Agriculture and Technology, Tokyo⁴²Toyama National College of Maritime Technology, Toyama⁴³University of Tsukuba, Tsukuba⁴⁴Utkal University, Bhubaneswer⁴⁵Virginia Polytechnic Institute and State University, Blacksburg, Virginia⁴⁶Yonsei University, Seoul

(Received 21 April 2001; published 22 August 2001)

We report observations of the Cabibbo suppressed decays $B \rightarrow D^{(*)}K^-$ using a 10.4 fb^{-1} data sample accumulated at the $\Upsilon(4S)$ resonance with the Belle detector at the KEKB e^+e^- storage ring. We find that the ratios of Cabibbo suppressed to Cabibbo favored branching fractions are $\mathcal{B}(B^- \rightarrow D^0 K^-)/\mathcal{B}(B^- \rightarrow D^0 \pi^-) = 0.079 \pm 0.009 \pm 0.006$, $\mathcal{B}(\bar{B}^0 \rightarrow D^+ K^-)/\mathcal{B}(\bar{B}^0 \rightarrow D^+ \pi^-) = 0.068 \pm 0.015 \pm 0.007$, $\mathcal{B}(B^- \rightarrow D^{*0} K^-)/\mathcal{B}(B^- \rightarrow D^{*0} \pi^-) = 0.078 \pm 0.019 \pm 0.009$, and $\mathcal{B}(\bar{B}^0 \rightarrow D^{*+} K^-)/\mathcal{B}(\bar{B}^0 \rightarrow D^{*+} \pi^-) = 0.074 \pm 0.015 \pm 0.006$. These are the first observations of the $B \rightarrow D^+ K^-$, $D^{*0} K^-$, and $D^{*+} K^-$ decay processes.

DOI: 10.1103/PhysRevLett.87.111801

PACS numbers: 13.25.Hw, 12.15.Hh

Comprehensive tests of the standard model mechanism for CP violation will ultimately require measurements of the ϕ_3 angle of the Kobayashi-Maskawa unitarity triangle [1]. For this, many authors have proposed the measurement of direct CP -violating asymmetries due to the interference between $b \rightarrow c$ and $b \rightarrow u$ transition amplitudes in the Cabibbo suppressed $B^- \rightarrow D^0 K^-$ channel as a theoretically clean way to determine ϕ_3 [2]. As a first step in this program, it is necessary to establish that the Cabibbo suppressed decay modes exist and occur at the expected rates.

In the tree-level approximation, the branching fractions for the Cabibbo suppressed decay processes $B \rightarrow D^{(*)}K^-$ are related to those for their $B \rightarrow D^{(*)}\pi^-$ counterparts [3] by

$$R \equiv \frac{\mathcal{B}(B \rightarrow D^{(*)}K^-)}{\mathcal{B}(B \rightarrow D^{(*)}\pi^-)} \simeq \tan^2 \theta_C (f_K/f_\pi)^2 \simeq 0.074. \quad (1)$$

Here θ_C is the Cabibbo angle, and f_K and f_π are the meson decay constants. The only Cabibbo suppressed $B \rightarrow DK$ decay observed to date is $B^- \rightarrow D^0 K^-$, which is reported by the CLEO group to have a ratio of branching fractions $R = \mathcal{B}(B^- \rightarrow D^0 K^-)/\mathcal{B}(B^- \rightarrow D^0 \pi^-) = 0.055 \pm 0.014 \pm 0.005$ [4], in agreement with expectations.

In this paper, we report the first observations of the Cabibbo suppressed processes $B^- \rightarrow D^{*0} K^-$, $\bar{B}^0 \rightarrow D^{*+} K^-$, and $\bar{B}^0 \rightarrow D^+ K^-$, and a new measurement of $B^- \rightarrow D^0 K^-$, using data collected at the $\Upsilon(4S)$ resonance with the Belle detector [5] at the KEKB asymmetric energy e^+e^- collider [6]. The good high momentum particle identification capability of the Belle detector enables us to extract signals for $B \rightarrow D^{(*)}K^-$ that are well separated from the more abundant, Cabibbo favored $B \rightarrow D^{(*)}\pi^-$ processes. The results are based on a 10.4 fb^{-1} data sample that contains $11.1 \times 10^6 B\bar{B}$ pairs.

Belle is a general-purpose detector which includes a 1.5 T superconducting solenoid magnet. Charged particle tracking covering approximately 90% of the total center of mass (cm) solid angle is provided by a silicon vertex detector, consisting of three nearly cylindrical layers of double-sided silicon strip detectors, and a 50-layer central drift chamber (CDC). Particle identification is accomplished by combining the responses from a silica aerogel Čerenkov counter (ACC) and a time of flight (TOF) counter system with specific ionization (dE/dx) measurements in the CDC. The combined response of the three systems provides K/π separation of at least “ 2.5σ equivalent” for laboratory momenta up to $3.5 \text{ GeV}/c$. To distinguish the *prompt* kaons and pions in $B \rightarrow D^{(*)}h^-$ ($h^- = K^-$ or π^-) decays, only the ACC and dE/dx are used since

the TOF system provides no significant kaon and pion separation at momenta relevant to this analysis. A CsI electromagnetic calorimeter located inside the solenoid coil is used for γ/π^0 detection.

The $B \rightarrow D^{(*)}K^-$ processes have kinematic properties nearly identical to those of $B \rightarrow D^{(*)}\pi^-$ decays. While the latter processes produce the most significant backgrounds, they also provide control samples that are used to establish cuts on kinematic variables, determine the experimental resolutions, evaluate the systematic errors, and normalize the results.

In this analysis, we require, except for the $K_S \rightarrow \pi^+\pi^-$ decay daughters, that the charged tracks have a point of closest approach to the interaction point within ± 5 mm in the direction perpendicular and ± 5 cm in the direction parallel to the beam axis. For each charged track, the particle identification system is used to determine a K/π likelihood ratio $P(K/\pi)$ that ranges between 0 (likely to be π) and 1 (likely to be K). We form candidate D^0 mesons using the $K^-\pi^+$, $K^-\pi^+\pi^0$, and $K^-\pi^+\pi^+\pi^-$ decay modes, and D^+ mesons using $K^-\pi^+\pi^+$, $K_S\pi^+$, $K_S\pi^+\pi^+\pi^-$, and $K^-K^+\pi^+$ decays. (The inclusion of charge conjugate states is implied throughout this paper.) For the assignment of charged kaons from D decays, we require $P(K/\pi) > 0.3$ in reconstructing $D^0 \rightarrow K^-\pi^+$ and all other D^0 decay modes associated with $D^{*+} \rightarrow D^0\pi^+$; otherwise we require $P(K/\pi) > 0.7$. Candidate π^0 mesons are reconstructed from pairs of γ 's, each with energy greater than 30 MeV, that have an invariant mass in the range of $\pm 2\sigma$ ($\sigma = 5.3$ MeV/ c^2) of the measured π^0 mass value and magnitude of the total three momentum greater than 200 MeV/ c . For the slow π^0 from the $D^* \rightarrow D\pi^0$ decay we require only that its invariant mass be in the range between -14.4 and $+10.8$ MeV of the π^0 mass (this corresponds to a $\pm 2\sigma$ cut). The $K_S \rightarrow \pi^+\pi^-$ candidates are reconstructed from two oppositely charged tracks that form an invariant mass within $\pm 3\sigma$ ($\sigma = 4.6$ MeV/ c^2) of the measured K_S mass value with a vertex which is displaced at least 2 mm from the interaction point in the direction of the K_S momentum. The selected π^0 and K_S candidates are kinematically constrained to their nominal mass values.

For each D -meson decay topology, we select particle combinations that have a reconstructed invariant mass within $\pm 2.5\sigma_D$ of the measured D mass value, where σ_D is the D mass resolution, which varies from 5 to 13 MeV/ c^2 depending on the decay mode. The D candidates are then subjected to a mass-constrained kinematic fit. For all modes except for $D^+ \rightarrow K_S\pi^+$, we further reduce backgrounds by a selection on the quality of the vertex fit.

For D^{*0} and D^{*+} candidates, we use the $D^{*0} \rightarrow D^0\pi^0$, and $D^{*+} \rightarrow D^0\pi^+$ and $D^+\pi^0$ decay channels. We select events where the mass difference between the $D\pi$ and D particle combinations is within $\pm 3\sigma$ of the expected

value for $D^{*+} \rightarrow D^0\pi^+$, and $\pm 2\sigma$ for $D^{*0} \rightarrow D^0\pi^0$ and $D^{*+} \rightarrow D^+\pi^0$. A kinematic fit that constrains the D^* mass to its nominal value is applied to the events that satisfy the selection criteria.

When we isolate $B \rightarrow D^{(*)}h^-$ candidates, we use a quantity we call the *lab constrained mass*, M_{lc} , which is the $D^{(*)}h^-$ invariant mass calculated with the assumption of two equal-mass particles from laboratory momenta: $M_{lc} = \sqrt{(E_B^{lab})^2 - (p_B)^2}$, where p_B is the B candidate's laboratory momentum and $E_B^{lab} = \frac{1}{E_{ee}}(s/2 + \mathbf{P}_{ee} \cdot \mathbf{P}_B)$, where s is the square of the cm energy, \mathbf{P}_B is the laboratory momentum vector of the B meson candidate, and \mathbf{P}_{ee} and E_{ee} are the laboratory momentum and energy of the e^+e^- system, respectively. To identify $B \rightarrow D^{(*)}K^-/D^{(*)}\pi^-$ samples we use the cm *energy difference*, which is defined as $\Delta E = E_{D^{(*)}}^{cm} + E_{\pi^-}^{cm} - E_{beam}^{cm}$, where $E_{D^{(*)}}^{cm}$ is the cm energy of the $D^{(*)}$ candidate and $E_{\pi^-}^{cm}$ is the cm energy of the prompt h^- track calculated *assuming the pion mass* and E_{beam}^{cm} is the cm beam energy. With this pion mass assumption, $B \rightarrow D^{(*)}\pi^-$ events peak at $\Delta E = 0$, while the $D^{(*)}K^-$ peak is shifted to $\Delta E = -49$ MeV. Typical ΔE resolutions obtained for $B \rightarrow D^{(*)}\pi^-$ and $B \rightarrow D^{(*)}K^-$ are 16 and 19 MeV, respectively; hence we can distinguish these two processes by the ΔE distribution. For further analysis we accept B candidates with $5.27 < M_{lc} < 5.29$ GeV/ c^2 and $-0.2 < \Delta E < 0.2$ GeV.

In the case of multiple entries from one event, we choose the one with the smallest value of a χ^2 that is determined

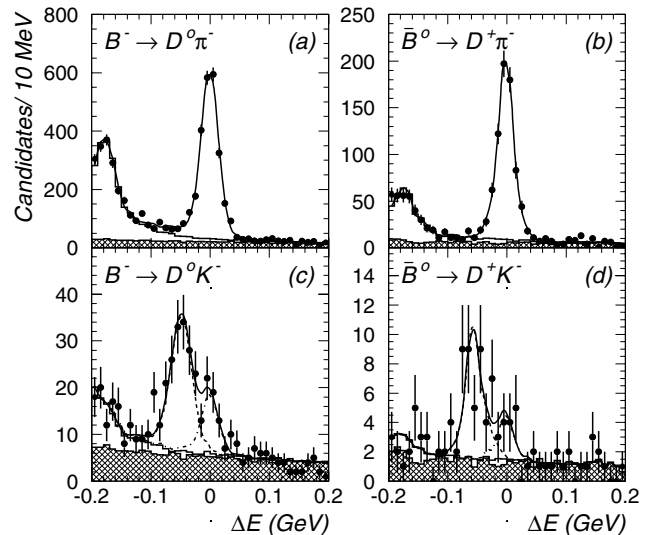


FIG. 1. The ΔE distributions for the (a) $B^- \rightarrow D^0\pi^-$ and (b) $\bar{B}^0 \rightarrow D^+\pi^-$ samples, and the (c) $B^- \rightarrow D^0K^-$ and (d) $\bar{B}^0 \rightarrow D^+K^-$ enriched samples, where in each case a pion mass is assigned to the π^-/K^- track candidate. The points with error bars are the data; the curves show the results of fits that are described in the text. The open histograms are the sums of background functions scaled to fit the data, and the hatched histogram indicates the continuum component of the background.

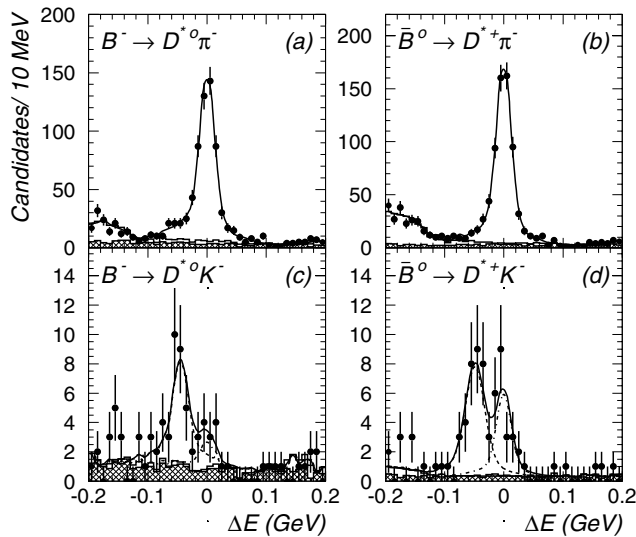


FIG. 2. The ΔE distributions for the (a) $B^- \rightarrow D^{*0} \pi^-$ and (b) $\bar{B}^0 \rightarrow D^{*+} \pi^-$ control samples, and the (c) $B^- \rightarrow D^{*0} K^-$ and (d) $\bar{B}^0 \rightarrow D^{*+} K^-$ enriched samples, where in each case a pion mass is assigned to the π^-/K^- track candidate. The curves and histograms are the same as those in Fig. 1.

from the differences between measured and nominal values of M_D , M_{1c} and, when appropriate, $M_{D^*} - M_D$ and M_{π^0} . For the latter, we consider only the π^0 from $D^{*0} \rightarrow D^0 \pi^0$ and $D^{*+} \rightarrow D^+ \pi^0$ decays. Background events from $e^+ e^- \rightarrow q\bar{q}$ continuum processes are reduced using the ratio of the second-to-zeroth Fox-Wolfram moments [7], R_2 , and the angle between the sphericity axis of the B candidate and the sphericity axis of the rest of the particles in the event, θ_{sph} . For $D^0 \rightarrow K^- \pi^+$ decays and all modes with $D^{*+} \rightarrow D^+ \pi^+$, since continuum backgrounds are small we require only $R_2 < 0.5$. This cut retains 96% of the signal and rejects 25% of the continuum. For all other modes, we impose the additional requirement of $|\cos\theta_{\text{sph}}| < 0.75$, which retains 75% of the signal and rejects 80% of the continuum events.

We extract $B \rightarrow D^{(*)} K^-$ enriched samples by applying a stringent particle identification condition on the prompt h^- , namely, $P(K/\pi) > 0.8$; $B \rightarrow D^{(*)} \pi^-$ samples are selected with a criterion $P(K/\pi) < 0.8$. The ΔE distributions for the $B \rightarrow D \pi^-$ and $B \rightarrow DK^-$ enriched samples are shown in Figs. 1(a) and 1(b), and 1(c) and 1(d), respectively. The corresponding distributions for the D^* channels are shown in Figs. 2(a)–2(d).

Kaon and pion identification efficiencies $\varepsilon(K)$ and $\varepsilon(\pi)$ are experimentally determined from a kinematically selected sample of high momentum $D^{*+} \rightarrow D^0 \pi^+$, $D^0 \rightarrow K^- \pi^+$ decays where the K^- and π^+ mesons from D^0 candidates are in the same cm momentum (p^{cm}) and angular region as the prompt h^- particle in $B \rightarrow D^{(*)} h^-$ decay ($2.1 < p^{\text{cm}} < 2.5$ GeV/c). With our $P(K/\pi)$ cut value of 0.8, the efficiencies are $\varepsilon(K) = 0.765 \pm 0.006$ and $\varepsilon(\pi) = 0.980 \pm 0.003$, and the $\pi \rightarrow K$ misidentification rate is $2.0 \pm 0.3\%$.

In Figs. 1(c), 1(d), 2(c), and 2(d), the peaks around $\Delta E = -49$ MeV correspond to $B \rightarrow D^{(*)} K^-$ decays while the peaks around $\Delta E = 0$ are due to feed across from misidentified $D^{(*)} \pi^-$ decays. The area of the feed-across peak is 2.0% of the $D^{(*)} \pi^-$ signal yield [observed in Figs. 1(a), 1(b), 2(a), and 2(b)], which is consistent with the $\pi \rightarrow K$ misidentification rate.

We determine the numbers of $D^{(*)} \pi^-$ events and the line shape parameters by fitting the ΔE distributions for the $D^{(*)} \pi^-$ samples of Figs. 1(a), 1(b), 2(a), and 2(b). We represent the signal distributions using two Gaussian functions with different central values and widths. The background has two components. One is due to contributions from $D\rho^-$, $D^*\rho^-$, and other B -meson decay modes [8], which produce the complicated structures mostly seen at negative values of ΔE , and the other is due to continuum events, which populate the entire ΔE region. The shapes of the $B\bar{B}$ backgrounds are histograms determined using Monte Carlo (MC) simulated events [9]. The shapes of the continuum backgrounds are histograms taken from the ΔE distributions for events in the M_{1c} sideband regions ($5.20 < M_{1c} < 5.26$ GeV/c²). In the fit to the $D^{(*)} \pi^-$ sample ΔE distributions, we allow the peak positions, widths, and normalization of the signal functions to vary, as well as the normalization of both the $B\bar{B}$ and the continuum background contributions. The fit results are shown in Figs. 1(a), 1(b), 2(a), and 2(b) as solid curves. The resulting numbers of $D^{(*)} \pi^-$ events are given in Table I.

In the fits to the $D^{(*)} K^-$ enriched ΔE distributions, the parameters of the two Gaussians for the $D^{(*)} K^-$ signal are fixed at the values determined from separate fits (not shown here) to the $D^{(*)} \pi^-$ samples with a kaon mass hypothesis applied to the prompt hadron track. The $D^{(*)} K^-$ peak position with the pion mass hypothesis is then given by reversing the relative position of the $D^{(*)} \pi^-$ signal with the kaon mass hypothesis with respect to its original position.

TABLE I. The fit results for the numbers of $D^{(*)} \pi^-$ and $D^{(*)} K^-$ events, the feed across from $D^{(*)} \pi^-$ to $D^{(*)} K^-$ enriched sample, and the statistical significance of the $D^{(*)} K^-$ signal.

	$D^{(*)} \pi^-$ Events	$D^{(*)} K^-$ Events	$D^{(*)} \pi^-$ Feed across	Stat. Sig.
$B^- \rightarrow D^0 h^-$	2402.8 ± 97.8	138.4 ± 15.5	52.0 ± 11.4	11.7
$\bar{B}^0 \rightarrow D^+ h^-$	681.9 ± 32.1	33.7 ± 7.3	10.4 ± 4.9	6.1
$B^- \rightarrow D^{*0} h^-$	584.8 ± 32.4	32.8 ± 7.8	6.8 ± 4.9	5.8
$\bar{B}^0 \rightarrow D^{*+} h^-$	640.9 ± 30.8	36.0 ± 7.1	21.0 ± 5.7	7.6

TABLE II. The resulting branching fraction ratio measurements. The first error is statistical and the second is systematic.

$\mathcal{B}(B^- \rightarrow D^0 K^-)/\mathcal{B}(B^- \rightarrow D^0 \pi^-)$	$= 0.079 \pm 0.009 \pm 0.006$
$\mathcal{B}(\bar{B}^0 \rightarrow D^+ K^-)/\mathcal{B}(\bar{B}^0 \rightarrow D^+ \pi^-)$	$= 0.068 \pm 0.015 \pm 0.007$
$\mathcal{B}(B^- \rightarrow D^{*0} K^-)/\mathcal{B}(B^- \rightarrow D^{*0} \pi^-)$	$= 0.078 \pm 0.019 \pm 0.009$
$\mathcal{B}(\bar{B}^0 \rightarrow D^{*+} K^-)/\mathcal{B}(\bar{B}^0 \rightarrow D^{*+} \pi^-)$	$= 0.074 \pm 0.015 \pm 0.006$

This procedure accounts for the kinematic shifts and smearing of the ΔE peaks caused by the incorrect mass assignment. The shape parameters for the feed across from $D^{(*)}\pi^-$ are determined from the $D^{(*)}\pi^-$ fits.

To determine the signal yield for the Cabibbo suppressed modes, we then perform fits to the ΔE distributions which are calculated with the pion mass assumption. The areas of the $D^{(*)}K^-$ signal and functions for the $D^{(*)}\pi^-$ feed across and the scaling factors of the continuum background shapes are allowed to vary. The $B\bar{B}$ background in the $D^{(*)}K^-$ enriched sample has two components: modes which also contribute to the $D^{(*)}\pi^-$ sample with one track misidentified as a high momentum kaon and other Cabibbo suppressed modes. The normalization of the feed across from the first component is fixed to the fit result for the $B\bar{B}$ background in the $D^{(*)}\pi^-$ sample multiplied by the measured pion misidentification rate. The contributions from other $D^{(*)}K^{(*)}$ modes are determined from a Monte Carlo simulation assuming that the branching fractions of the Cabibbo suppressed modes relative to the corresponding $D^{(*)}\pi^-/D^{(*)}\rho^-$ modes are reduced by the usual Cabibbo factor. The fit results are shown as solid curves in Figs. 1(c), 1(d), 2(c), and 2(d). The numbers of events in the $D^{(*)}K^-$ signal and $D^{(*)}\pi^-$ feed-across peaks are listed in Table I. Also listed in Table I are the statistical significance values for the $D^{(*)}K^-$ signals. For each channel, the statistical significance of the signal corresponds to at least 5 standard deviations.

Experimentally, the ratio of branching fractions is given by

$$R = \frac{N(B \rightarrow D^{(*)}K^-)}{N(B \rightarrow D^{(*)}\pi^-)} \times \frac{\eta(D^{(*)}\pi^-)}{\eta(D^{(*)}K^-)} \times \frac{\varepsilon(\pi)}{\varepsilon(K)},$$

where N and η denote the numbers of events and detection efficiencies for the indicated processes, and ε 's are the prompt pion and kaon identification efficiencies, respectively. The signal detection efficiencies are determined using MC, and $\eta(D^{(*)}K^-)$ are approximately 5% lower than $\eta(D^{(*)}\pi^-)$ due to the decay in flight of kaons. Particle identification efficiencies are determined from data as described earlier.

Since the kinematics of the $B \rightarrow D^{(*)}K^-$ and $B \rightarrow D^{(*)}\pi^-$ processes are quite similar, most of the systematic effects cancel in the ratios of branching fractions. The main sources of systematic error that do not cancel are the uncertainties in K/π identification efficiencies and the shape of the background in the ΔE distributions. Using

MC simulations, we estimate the systematic error in the K identification due to differences in the angle-momentum correlations of the D^{*+} and signal samples to be 2%. To estimate the systematic error due to the parametrization of the ΔE distributions, we use several different methods of fitting. These include using linear background functions, fixing the normalization of the $B\bar{B}$ backgrounds to the value predicted by MC, and forcing the parameters of $D^{(*)}K^-$ and/or $D^{(*)}\pi^-$ signals to deviate from their optimal values by $\pm 1\sigma$. As an additional check on the $D^{(*)}K^-$ signal parameters, we perform a fit using signal parameters determined from MC simulation. This fit is also consistent with the result from the nominal fit. The quadratic sums of those values are used as measures of the systematic errors from ΔE fitting. Compared to these, which range from 7.5% to 10.8%, other sources of systematic errors are determined to be negligibly small. The total systematic error for each channel is taken to be the sum in quadrature of the individual components.

The resulting R ratio measurements are listed with their statistical and systematic errors in Table II. For the $B \rightarrow D^+K^-$, $D^{*0}K^-$, and $D^{*+}K^-$ decay processes, these are first measurements. In all cases, the R ratios are consistent with the expected value given in Eq. (1).

In summary, by taking advantage of the good high momentum particle identification capability of Belle, we have observed signals for the Cabibbo suppressed decays $B \rightarrow D^0K^-$, D^+K^- , $D^{*0}K^-$, and $D^{*+}K^-$ that are well separated from the more abundant Cabibbo favored $B \rightarrow D^{(*)}\pi^-$ processes. We report values for the ratios of branching fractions $R = \mathcal{B}(B \rightarrow D^{(*)}K^-)/\mathcal{B}(B \rightarrow D^{(*)}\pi^-)$ that agree, within errors, with naive model calculation.

We wish to thank the KEKB accelerator group for the excellent operation of the accelerator. We acknowledge support from the Ministry of Education, Science, Sports and Culture of Japan and the Japan Society for the Promotion of Science; the Australian Research Council and the Australian Department of Industry, Science and Resources; the Department of Science and Technology of India; the BK21 program of the Ministry of Education of Korea, SRC program of the Korea Science and Engineering Foundation, and the Basic Science program of the Korea Research Foundation; the Polish State Committee for Scientific Research under Contract No. 2P03B 17017; the Ministry of Science and Technology of Russian Federation; the National Science Council and the Ministry of Education of Taiwan; the Japan-Taiwan Cooperative

Program of the Interchange Association; and the U.S. Department of Energy.

-
- [1] M. Kobayashi and K. Maskawa, *Prog. Theor. Phys.* **49**, 652 (1973).
- [2] M. Gronau and D. Wyler, *Phys. Lett. B* **265**, 172 (1991); I. Dunietz, *Phys. Lett. B* **270**, 75 (1991); D. Atwood, I. Dunietz, and A. Soni, *Phys. Rev. Lett.* **78**, 3257 (1997).
- [3] This relation assumes the validity of factorization and flavor-SU(3) symmetry. The numerical value is determined from adjusting the measured result for the ratio $\tau^- \rightarrow K^- \nu$ and $\pi^- \nu$ decays corrected for the phase space effect.
- [4] CLEO Collaboration, M. Athanas *et al.*, *Phys. Rev. Lett.* **80**, 5493 (1998).
- [5] Belle Collaboration, KEK Progress Report No. 2000-4 (to be published).
- [6] KEKB B-Factory Design Report, KEK Report No. 95-7, 1995; Y. Funakoshi *et al.*, in *Proceedings of the 2000 European Particle Accelerator Conference, Vienna, 2000* (Austrian Academy of Science Press, Vienna, 2000).
- [7] G. Fox and S. Wolfram, *Phys. Rev. Lett.* **41**, 1581 (1978).
- [8] The ΔE plots for $D\pi^-$ and DK^- have additional background at negative ΔE values from $B \rightarrow D^*\pi^-$ decays.
- [9] "QQ—The CLEO Event Generator," <http://www.lns.cornell.edu/public/CLEO/soft/QQ> (unpublished).